

# COPY

## HEAT TRANSFER TO LONGITUDINAL LAMINAR FLOW

### BETWEEN CYLINDERS

By E. M. Sparrow, A. L. Loeffler, Jr.  
and H. A. Hubbard

Lewis Research Center  
National Aeronautics and Space Administration  
Cleveland, Ohio

NASA FILE COPY

loan expires on last  
date stamped on back cover.  
PLEASE RETURN TO

DIVISION OF RESEARCH INFORMATION  
AERONAUTICS  
AND SPACE ADMINISTRATION  
Washington 25, D.C.

N-81325

E-725

### ABSTRACT

Consideration is given to the fully developed heat transfer characteristics for longitudinal laminar flow between cylinders arranged in an equilateral triangular array. The analysis is carried out for the condition of uniform heat transfer per unit length. Solutions are obtained for the temperature distribution, and from these, Nusselt numbers are derived for a wide range of spacing-to-diameter ratios. It is found that as the spacing ratio increases, so also does the wall-to-bulk temperature difference for a fixed heat transfer per unit length. Corresponding to a uniform surface temperature around the circumference of a cylinder, the circumferential variation of the local heat flux is computed. For spacing ratios of 1.5 ~ 2.0 and greater, uniform peripheral wall temperature and uniform peripheral heat flux are simultaneously achieved. A simplified analysis which neglects circumferential variations is also carried out, and the results are compared with those from the more exact formulation.

### NOMENCLATURE

- A, B, ..., F constants in the temperature solution
- $c_p$  specific heat at constant pressure
- d cylinder diameter,  $2r_0$
- $d_e$  equivalent diameter, eq. (27)
- h heat transfer coefficient
- j summation index
- k thermal conductivity

Copy No. \_\_\_\_\_

W (1) \_\_\_\_\_

L \_\_\_\_\_

E \_\_\_\_\_

A \_\_\_\_\_

H \_\_\_\_\_

S \_\_\_\_\_

X

(T)

(T)

M	mass flow parameter, $(w/12\rho)/s^2 \left(-\frac{1}{\mu} \frac{dp}{dz}\right)$
m	summation index
N	normal direction
$Nu_d, Nu_{d_e}$	Nusselt number, $hd/k$ and $hd_e/k$ respectively
n	summation index
p	static pressure
Q	heat transfer rate per unit length from one cylinder
q	local heat transfer rate per unit area
q <sub>l</sub>	circumferential average of q, $Q/2\pi r_0$
r	radial coordinate; $r_0$ , cylinder radius; $r^*$ , outer radius of equivalent annulus
s	half spacing between centers of cylinders
T	temperature; $T_w$ , wall temperature, $T_b$ , bulk temperature; $T_0$ , entering fluid temperature
u	axial velocity distribution
w	mass rate of flow associated with one cylinder
z	axial coordinate measuring distance from the entrance of the passage
$\delta_j$	dimensionless coefficients in velocity solution
$\theta$	angular coordinate
$\mu$	absolute viscosity
$\rho$	density
$\omega_j$	dimensionless coefficients in temperature solution

#### INTRODUCTION

In a previous investigation (ref. 1), consideration was given to the longitudinal laminar flow between cylinders arranged in regular array. Here, attention is directed to analyzing the heat transfer characteristics of such a

E-725

flow. This configuration has potential application in compact heat exchangers and has been frequently considered in connection with the cores of nuclear reactors.

A schematic diagram of the system under study is shown in Fig. 1. The cylindrical rods between which the fluid flows are arranged in equilateral triangular array, and the flow is laminar and full-developed. The thermal situation to be considered here is the condition of uniform heat transfer along the length of the passage. The goal of this analysis is to determine the fully-developed heat transfer characteristics of the problem, taking into account the circumferential variations of the temperature distribution which inevitably arise in the cross section of a noncircular passage. The existence of such peripheral variations is what makes the problem both interesting and challenging. The starting point of the study is the basic law of energy conservation appropriate to the three-dimensional situation. Solutions are found for a wide range of spacing to diameter ratios, and corresponding heat transfer results are obtained. For large spacings, the flow about any given cylinder should be little influenced by the presence of neighboring cylinders. With this in mind, a simplified analysis has been carried out neglecting circumferential variations, and the heat transfer results thus obtained are compared with those from the more complete formulation.

### ANALYSIS

Mathematical formulation. - To predict the heat transfer characteristics from first principles, we must begin with the fundamental physical law of energy conservation. The mathematical representation of this law appropriate to a fully developed flow may be written in cylindrical coordinates as follows

$$\rho c_p u \frac{\partial T}{\partial z} = k \left( \frac{\partial^2 T}{\partial r^2} + \frac{1}{r} \frac{\partial T}{\partial r} + \frac{1}{r^2} \frac{\partial^2 T}{\partial \theta^2} + \frac{\partial^2 T}{\partial z^2} \right) \quad (1)$$

where  $u$ , the axial velocity, depends on both cross section coordinates  $r$  and  $\theta$ .

PL-725

To facilitate applying Eq. (1) to the system under study, we refer to Fig. 2. The left hand sketch is a cross-sectional view. From the symmetry of the situation, it is easy to see that consideration need be given only to the typical 30° element which is blackened in the sketch. Once the solution is known within this element, then it is known everywhere throughout the cross section. An enlarged view of the typical element is shown at the right, along with the boundary conditions and dimensional nomenclature. The condition that the normal derivative be zero is an expression of symmetry. On the inner boundary,  $r = r_0$ , the temperature is assigned a value  $T_w$  which is independent of angle. Physically speaking, this means that the surface temperature is uniform around the circumference in a given cross section, although it will vary along the length. Of course, there still remains a circumferential temperature variation within the fluid and this will be included in the analysis. Before leaving the boundary conditions, it is interesting to observe that the case of uniform peripheral surface temperature is one of two interesting limiting conditions.\* The other, uniform peripheral heat flux, still remains to be analyzed.

The first step in attacking Eq. (1) is to introduce the condition of fully-developed heat transfer. For the case of uniform heat transfer per unit length, this condition is

$$\frac{\partial T}{\partial z} = \text{constant} = \frac{Q}{wc_p} = \frac{(Q/12)}{(w/12)c_p} \quad (2)$$

where  $w$  and  $Q$  respectively represent the mass flow and the heat transfer per unit length associated with a single cylinder in the array; while  $(w/12)$  and  $Q/12$  are the quantities appropriate to the typical 30° element of Fig. 2.

---

\* A thorough discussion of thermal boundary conditions in noncircular ducts is given in Ref. 2.

E-725

Next, it is necessary to know the velocity distribution  $u$ . In Ref. 1, a very accurate, but approximate solution for the velocity has been derived in the form

$$\frac{u}{s^2 \left( -\frac{1}{\mu} \frac{dp}{dz} \right)} = \frac{\sqrt{3}}{\pi} \ln \frac{r}{r_0} - \frac{1}{4} \left[ \left( \frac{r}{s} \right)^2 - \left( \frac{r_0}{s} \right)^2 \right] + \sum_{n=1}^{\infty} \frac{\delta_n}{6n} \left[ \left( \frac{r}{s} \right)^{6n} - \frac{r_0^{12n}}{r^{6n} s^{6n}} \right] \cos 6n\theta \quad (3)$$

The coefficients  $\delta_1$  through  $\delta_7$  have been tabulated to four decimal places in the reference for a wide range of spacing ratios, and additional significant figures were available when needed in the heat transfer analysis. Another piece of information which is needed from the velocity solution is the relation between the mass flow  $w$  and the pressure drop. For convenience, we define a dimensionless grouping  $M$  as\*

$$M \equiv \frac{(w/12\rho)}{s^4 \left( -\frac{1}{\mu} \frac{dp}{dz} \right)} \quad (4)$$

Numerical values of  $M$  may be obtained as a function of spacing ratio from Fig. 6 of Ref. 1.

Then, the information contained in Eqs. (2) through (4) may be introduced into the energy Eq. (1). After rearrangement, the governing equation for  $T$  is found to be

$$\frac{\partial^2 T}{\partial r^2} + \frac{1}{r} \frac{\partial T}{\partial r} + \frac{1}{r^2} \frac{\partial^2 T}{\partial \theta^2} = \frac{Q/12k}{Ms^2} \left\{ \frac{\sqrt{3}}{\pi} \ln \frac{r}{r_0} - \frac{1}{4} \left[ \left( \frac{r}{s} \right)^2 - \left( \frac{r_0}{s} \right)^2 \right] + \sum_{n=1}^{\infty} \frac{\delta_n}{6n} \left( \frac{r}{s} \right)^{6n} \left[ 1 - \left( \frac{r_0}{r} \right)^{12n} \right] \cos 6n\theta \right\} \quad (5)$$

Solution of the governing equation. - In approaching Eq. (5), we look for particular and homogeneous solutions. Thus, the solution for  $T$  is expressed as the sum of these separate solutions as follows

$$T = T_p + T_h \quad (6)$$

---

\*In Ref. 1, the symbol  $Q$  is used to denote  $w/12\rho$ .

E-725

For a particular solution, any function satisfying Eq. (5) will suffice. It is easily verified by direct substitution that the following expression is a satisfactory particular solution

$$T_p = \frac{(Q/12k)r^2}{Ms^2} \left\{ -\frac{\sqrt{3}}{4\pi} + \frac{1}{16} \left(\frac{r_0}{s}\right)^2 - \frac{1}{64} \left(\frac{r}{s}\right)^2 + \frac{\sqrt{3}}{4\pi} \ln \frac{r}{r_0} + \sum_{n=1} \frac{\delta_n}{24n} \left(\frac{r}{s}\right)^{6n} \left[ \frac{1}{6n+1} + \frac{(r_0/r)^{12n}}{6n-1} \right] \cos 6n\theta \right\} \quad (7)$$

To find the homogeneous equation, we set the right side of Eq. (5) equal to zero and get

$$\frac{\partial^2 T_h}{\partial r^2} + \frac{1}{r} \frac{\partial T_h}{\partial r} + \frac{1}{r^2} \frac{\partial^2 T_h}{\partial \theta^2} = 0$$

This is the well-known Laplace equation, the solution to which may be found in various books on advanced calculus as

$$T_h = A + B \ln r + \sum_m (C_m r^m + D_m r^{-m})(E_m \cos m\theta + F_m \sin m\theta) \quad (8)$$

where  $m$  takes on integral values to insure that  $T$  is single valued, i.e., that  $T(\theta) = T(\theta + 2\pi)$ . The constants  $A, B, \dots, F$  remain to be determined from the boundary conditions.

So, the general solution of Eq. (5) is given by Eq. (6) in conjunction with  $T_p$  and  $T_h$  from (7) and (8). But, to complete the solution, there still remains the task of satisfying the boundary conditions. Starting with the most easily applied conditions, we first impose the symmetry requirement that  $\partial T / \partial \theta = 0$  at  $\theta = 0^\circ$  and at  $\theta = 30^\circ$  (see fig. 2(b)). After differentiating Eq. (6) and substituting from (7) and (8), it is found that the condition at  $\theta = 0^\circ$  yields

$$F_m \equiv 0 \quad (9)$$

while from the condition at  $\theta = 30^\circ$ , it follows that

$$m = 6, 12, 18, \dots \quad (10)$$

to insure that  $\sin n\pi/6 = 0$ . With this information, it is convenient to rephrase the temperature solution (6) as

$$T = T_p + A + B \ln r + \sum_{j=1}^{\infty} (C_j r^{6j} + D_j r^{-6j}) \cos 6j\theta \quad (11)$$

where  $T_p$  is still given by Eq. (7) and  $E_j$  has been set equal to unity without loss of generality.

Next, it is required that at the surface of the cylinder,  $r = r_0$ , the temperature take on the value  $T_w$  independent of angle. Applying this condition to Eq. (11), it is found that

$$A = T_w - B \ln r_0 - \frac{(Q/12k)r_0^2}{Ms^2} \left\{ -\frac{\sqrt{3}}{4\pi} + \frac{3}{64} \left(\frac{r_0}{s}\right)^2 \right\} \quad (12a)$$

$$D_j = -C_j r_0^{12j} - \frac{(Q/12k)}{Ms^2} \frac{\delta_n}{2(36n^2 - 1)} \frac{r_0^{12n+2}}{s^{6n}}, \quad n = j \quad (12b)$$

Further, to make certain that energy conservation is satisfied on an overall basis for the typical element of Fig. 2(b), we equate the heat transfer per unit length,  $Q/12$ , to the heat conducted at the surface of the cylinder, i.e.,

$$Q/12 = \int_0^{\pi/6} -k \left( \frac{\partial T}{\partial r} \right)_{r_0} r_0 d\theta \quad (13)$$

This insures that there is no net energy transport across the other boundaries of the typical element. Of course, overall energy would be automatically satisfied by an exact solution; but if an approximate solution is being contemplated, then it must be imposed as a separate requirement. Inserting Eq. (11) into the overall conservation condition (13) gives

$$B = \frac{Q/12k}{Ms^2} \left[ -\frac{6Ms^2}{\pi} + \frac{\sqrt{3}}{4\pi} r_0^2 - \frac{1}{16} \frac{r_0^4}{s^2} \right] \quad (14)$$

Before going ahead to the final boundary condition, it is useful to bring together the findings of the previous paragraph. Introducing Eqs. (12) and (14) into the temperature solution (11) and substituting for  $T_p$  from Eq. (7)

E-725

gives

$$\begin{aligned}
 T - T_w = & \frac{Q/12k}{Ms^2} \left\{ \left[ \frac{\sqrt{3}}{4\pi} (r^2 + r_o^2) - \frac{1}{16} \frac{r_o^4}{s^2} - \frac{6Ms^2}{\pi} \right] \ln \frac{r}{r_o} - \frac{1}{64} \frac{(r^4 - r_o^4)}{s^2} \right. \\
 & + \left. \left[ -\frac{\sqrt{3}}{4\pi} + \frac{1}{16} \left( \frac{r_o}{s} \right)^2 \right] (r^2 - r_o^2) \right\} + \sum_{j=1} C_j r^{6j} \left[ 1 - \left( \frac{r_o}{r} \right)^{12j} \right] \cos 6j\theta \\
 & + \frac{(Q/12k)r^2}{Ms^2} \sum_{n=1} \delta_n \cos 6n\theta \left\{ \frac{(r/s)^{6n}}{24n} \left[ \frac{1}{6n+1} + \frac{(r_o/r)^{12n}}{6n-1} \right] - \frac{(r_o/r)^2}{2(36n^2-1)} \frac{r_o^{12n}}{r^{6n}s^{6n}} \right\}
 \end{aligned} \tag{15}$$

Remembering that  $\delta_n$  and  $M$  are known numerical constants whose values depend upon  $s/r_o$ , it is seen that the temperature distribution will be completely determined as soon as the  $C_j$  are found. At our disposal is the condition that  $\partial T / \partial N = 0$  on the right hand boundary of the typical element (see fig. 2(b)), on which  $r = s / \cos \theta$ . In applying this condition, it is convenient to use the identity

$$\frac{\partial T}{\partial N} = \frac{\partial T}{\partial r} \cos \theta - \frac{\partial T}{\partial \theta} \frac{\sin \theta}{r} \tag{16}$$

Then, introducing the temperature distribution (15) and setting  $\partial T / \partial N = 0$  for  $r = s / \cos \theta$ , there is obtained after considerable rearrangement

$$\begin{aligned}
 & \sum_{j=1} \omega_j (\cos \theta)^{1-6j} \left[ \cos(6j-1)\theta + \left( \frac{r_o \cos \theta}{s} \right)^{12j} \cos(6j+1)\theta \right] \\
 & = - \sum_{n=1} \delta_n \left\{ \frac{3n}{36n^2-1} \left( \frac{r_o}{s} \right)^{12n+2} (\cos \theta)^{6n+1} \cos(6n+1)\theta \right. \\
 & \quad + \frac{\cos(6n-1)\theta + (1/3n)\cos \theta \cos 6n\theta}{4(6n+1)(\cos \theta)^{6n+1}} \\
 & \quad \left. + \frac{(r_o/s)^{12n} (\cos \theta)^{6n-1}}{4(1-6n)} \left[ \cos(6n+1)\theta - (1/3n)\cos \theta \cos 6n\theta \right] \right\} \\
 & - \left[ -\frac{6M}{\pi} + \frac{\sqrt{3}}{4\pi} \left( \frac{r_o}{s} \right)^2 - \frac{1}{16} \left( \frac{r_o}{s} \right)^4 \right] \cos^2 \theta - \frac{1}{8} \left( \frac{r_o}{s} \right)^2 - \frac{\sqrt{3}}{2\pi} \ln \left( \frac{s}{r_o \cos \theta} \right) + \frac{1}{16 \cos^2 \theta} + \frac{\sqrt{3}}{4\pi}
 \end{aligned} \tag{17}$$

E-725



where

$$\omega_j = C_j \frac{6^j s^{6j} M}{(Q/12k)} \tag{17a}$$

The only unknowns appearing in Eq. (17) are the coefficients  $\omega_j$  (i.e.,  $C_j$ ). In considering ways of solving for the  $\omega_j$ , the first thought might be to use the Fourier series method. If workable, this procedure would provide an infinite number of  $\omega_j$  values while satisfying Eq. (17) at all points along the boundary,  $0^\circ \leq \theta \leq 30^\circ$ . However, Fourier methods cannot be applied in the present problem and some other approach must be used. The procedure employed here is as follows: First, the summation involving the  $\omega_j$  is truncated after  $i$  terms. Next, the condition (17) is applied successively at  $i$  values of  $\theta$  in the range  $0^\circ \leq \theta \leq 30^\circ$ . This yields  $i$  linear equations, each of which contains  $i$  unknown values of  $\omega_j$ . As soon as the  $s/r_0$  ratio is specified, the right hand side of each equation can be reduced to a numerical constant since the values of  $\delta_n$  and  $M$  are available from Ref. 1. So, there are  $i$  linear, inhomogeneous algebraic equations, the solution to which yields numerical values for the  $\omega_j$ . To check the accuracy of the results, the entire procedure may be reapplied using additional terms in the summation. From this, it is found that the additional terms do not significantly affect the numerical values of the first few coefficients. Another important fact is that the magnitudes of the  $\omega_j$  decrease quite rapidly with increasing  $j$ , so that only the first few  $\omega_j$  are really important. These favorable circumstances somewhat ease the task of finding a sufficient number of accurate  $\omega_j$  values. The numerical results which have been obtained for the  $\omega_j$  are listed in table I as a function of the spacing ratio  $s/r_0$ .

With the  $\omega_j$  values now known, then the coefficients  $C_j$  are also known through Eq. (17a). With these, we may return to the temperature distribution (15). For convenience, the summation involving the  $C_j$  may be rephrased as

E-725

$$\sum_{j=1} C_j r^{6j} \left[ 1 - \left( \frac{r_0}{r} \right)^{12j} \right] \cos 6j\theta = \frac{Q/12k}{M} \sum_{j=1} \frac{\omega_j \left( \frac{r}{s} \right)^{6j}}{6j} \left[ 1 - \left( \frac{r_0}{s} \right)^{12j} \right] \cos 6j\theta \quad (18)$$

Since  $\delta_n$  and  $M$  are also known numerical constants (ref. 1), then it is clear that once the geometrical parameters  $r_0$  and  $s$  have been specified, the temperature distribution within the typical elements is determined. So, we are now in a position to proceed with the determination of the heat transfer results.

### HEAT TRANSFER CHARACTERISTICS

Wall-to-bulk temperature difference and Nusselt number. - The solution which has just been presented gives the distribution of the temperature in a cross section relative to the wall temperature  $T_w$  in that cross section. So, to complete the solution, there still remains the task of finding  $T_w$ . Furthermore, in practice, it is the wall temperature itself which is usually the quantity of greatest practical interest, for example, on a materials limit or a thermal stress basis.

Now, in a situation where the wall heat flux is prescribed, the bulk temperature is immediately determined according to the following relation

$$T_b = T_0 + \frac{Q}{w c_p} z \quad (19)$$

where  $T_0$  is the temperature of the fluid at the entrance to the heated passage. Making use of this, the wall temperature may be written as

$$T_w \equiv T_b + (T_w - T_b) = T_0 + \frac{Q}{w c_p} z + (T_w - T_b) \quad (20)$$

From this, it is clear that the wall-to-bulk temperature difference ( $T_w - T_b$ ) is the key to the determination of the wall temperature. In addition, as soon as  $T_w - T_b$  is known, then Nusselt number results can be obtained.

To compute the wall-to-bulk temperature difference, we start with the standard definition of the bulk temperature

$$T_b \equiv \frac{\iint \text{Area} T_{pur} dr d\theta}{\iint \text{Area} \rho_{ur} dr d\theta} \quad (21)$$

The denominator is simply the mass flow. Specializing to the typical element of Fig. 2(b) and subtracting away the wall temperature, there is obtained

$$T_w - T_b = \frac{\rho \int_0^{30^\circ} \int_{r_o}^{s/\cos \theta} (T_w - T)ur dr d\theta}{w/12} \quad (22)$$

In evaluating the integrand, the velocity distribution is introduced from Eq. (3), while the temperature distribution is taken from Eq. (15) as modified by (18). After making these substitutions and rephrasing in terms of dimensionless variables, the following functional relation is revealed

$$\frac{T_w - T_b}{Q/12k} = f(s/r_o) \quad (23)$$

This is an interesting result in that the dependence on geometry enters only as the ratio  $s/r_o$ , rather than as  $s$  and  $r_o$  separately. It is easy to see that multiplying out the temperature and velocity distributions in the integrand of Eq. (22) leads to an exceedingly lengthy expression which is made even longer when the double integration is carried out. To display only the end result of the integration would require considerable space. In the interest of a concise presentation, the details associated with the evaluation of Eq. (22) will be omitted and only a few general remarks will be made as follows: In organizing the computations, separate account was kept of the contribution due to the non-series portion of  $u$  and  $T - T_w$  and of the contribution due to the series terms. As expected, the relative importance of the series terms increased as the spacing decreased. The integrations which arose in connection with Eq. (22) were carried out analytically as far as possible; however, it was ultimately necessary to compute some specific integrals by numerical means and these are

given in the Appendix with the hope that this information may be useful to others.

From the evaluation of Eq. (22), numerical results for the wall-to-bulk temperature difference have been obtained as a function of the spacing ratio  $s/r_0$ . These results will be reported in terms of the customary Nusselt number representation. First, a heat transfer coefficient is defined as

$$h \equiv \frac{Q}{\pi d(T_w - T_b)} = \frac{Q/12}{(\pi d/12)(T_w - T_b)} \tag{24}$$

Then, using the cylinder diameter as characteristic dimension, the Nusselt number becomes

$$Nu_d = \frac{hd}{k} = \left(\frac{12}{\pi}\right) \frac{Q/12k}{T_w - T_b} \tag{25}$$

It may be seen that the Nusselt number is essentially the reciprocal of the dimensionless bulk temperature parameter which has been displayed in Eq. (23). From this it follows that the Nusselt number depends only on the spacing ratio  $s/r_0$ . Utilizing the numerical values obtained from evaluating Eq. (22), a graph of  $Nu_d$  as a function of  $s/r_0$  has been prepared and is presented as the solid curve of Fig. 3 - left hand ordinate. It is seen from the figure that  $Nu_d$  monotonically increases as  $s/r_0$  decreases; and with this, it follows from Eq. (25) that the wall-to-bulk temperature difference is smaller at smaller spacings for a fixed heat input. This trend is in accord with physical reasoning.

Now, with the relation between heat transfer and temperature difference established by Fig. 3, we may return to the computation of the wall temperature variation as given by Eq. (20). Dividing through by  $Q/k$  and introducing Eq. (25), there is obtained

$$\frac{T_w - T_0}{Q/k} = \frac{z}{(w/\mu)Pr} + \frac{1}{\pi Nu_d} \tag{26}$$

E-725

At a fixed flow, the value of  $(T_w - T_o)/(Q/k)$  at a particular  $z$  will diminish as the spacing diminishes. But, there will, of course, be a price in pressure drop to be paid to maintain the fixed flow. On the other hand, at a fixed pressure drop,  $w$  will diminish with decreasing spacing; and so, under this condition, the two terms of Eq. (26) vary in opposite directions. The dependence of the flow rate on spacing ratio is more acute (see Fig. 6, ref. 1) than is that of the Nusselt number. So, for  $z$  values sufficiently large to establish fully-developed conditions, it would be expected that  $(T_w - T_o)/(Q/k)$  would increase with decreasing spacing when the pressure drop is fixed.

Before leaving this section, it may be worthwhile to discuss briefly two other aspects of the results. First, it may be of interest to compare the heat transfer performance with that for laminar flow inside a circular tube ( $Nu_d = 48/11$ ). If we ask for the same wall-to-bulk temperature difference at a given heat flux per unit length, then this is achieved at a spacing ratio of 2.03. The second topic relates to the equivalent diameter. It is reasonably well-accepted that for laminar flow, the use of the equivalent diameter as a characteristic dimension is not sufficient to remove the dependence of the heat transfer results upon geometrical parameters. However, in the present problem, we are in a position to once again check on this point. From the definition

$$d_e = \frac{4(\text{cross-sectional area})}{\text{heated perimeter}} \tag{27a}$$

it is easy to show that

$$\frac{d_e}{d} = \frac{6(s/r_o)^2}{\sqrt{3} \pi} - 1 \tag{27b}$$

Then, since  $Nu_{d_e} = (Nu_d)(d_e/d)$ , we may find the dependence of  $Nu_{d_e}$  upon  $s/r_o$  by using the results which have previously been presented. A curve derived in this way has been plotted as a solid line in Fig. 3 - right hand ordinate. It is seen that the geometrical factors involved in the equivalent

E-725

diameter have given  $Nu_{d_e}$  a completely opposite trend to that of  $Nu_d$ . However, the variation in  $Nu_{d_e}$  is not less than that experienced by  $Nu_d$ .

Peripheral variation of local heat transfer. - In the previous section,

attention has been focused on overall quantities such as the heat transfer per unit length, the bulk temperature and the Nusselt number. Here, consideration is given to the local heat transfer at various positions around the periphery of a cylinder.

Since the velocity distribution varies with angular position around a cylinder while the surface temperature is prescribed to be independent of angle, it is evident that there may be a circumferential variation of the local heat transfer.

To compute the local heat transfer, we use Fourier's law

$$q = -k \left( \frac{\partial T}{\partial r} \right)_{r_0} \tag{28}$$

where  $q$  represents the heat transfer per unit area. The temperature distribution is introduced from Eq. (15) as modified by (18) and after some rearrangement, it is found that

$$\frac{q}{\bar{q}} = 1 - \frac{\pi}{6M} \left\{ \sum_{j=1}^{\infty} 2\omega_j \left( \frac{r_0}{s} \right)^{6j} \cos 6j\theta + \sum_{n=1}^{\infty} \frac{\delta_n (r_0/s)^{6n+2}}{2(6n-1)} \cos 6n\theta \right\} \tag{29}$$

where  $\bar{q}$ , the mean local heat transfer, is related to the heat transfer per unit length  $Q$  by

$$\bar{q} = \frac{Q}{2\pi r_0} \tag{29a}$$

Utilizing the tabulated values of  $\omega_j$  from table I with the  $\delta_j$  and  $M$  from Ref. 1, the circumferential variation of  $q$  has been evaluated. The results are plotted on Fig. 4 as a function of  $\theta$  for parametric values of the spacing ratio  $s/r_0$ . By the symmetry considerations already mentioned in connection with Figs. 2(a) and (b), the variation over the entire circumference is known once the results for a typical  $30^\circ$  section have been given.

E-725

From Fig. 4, it is seen that for close spacings (small  $s/r_0$ ), there is a significant circumferential heat transfer variation; while for open spacings (large  $s/r_0$ ), the heat transfer is essentially uniform around the circumference. Clearly, for all spacing ratios of 2 or greater, there is essentially no distinction between the case of peripherally uniform wall temperature or peripherally uniform heat transfer. For many applications, this statement might be considered applicable even to spacing ratios as low as 1.5. The trend of decreasing peripheral variations with increasing spacing may be explained on physical grounds. For close spacings, a given cylinder is much influenced by the presence of its neighbors, with the result that the velocity distribution is circumferentially nonuniform and so is the heat transfer. As the spacing grows larger, the flow about a given cylinder is less disturbed by its neighbors. The resulting trend of the velocity toward axial symmetry is accompanied by a trend toward a more uniform surface heat transfer.

It is interesting to note that the largest heat transfer occurs at  $\theta = 30^\circ$ , the location of the largest open area for flow. On the other hand, the smallest heat transfer occurs at  $\theta = 0^\circ$ , which is the location of the smallest open area for flow. From this, it may be inferred that if the heat transfer were prescribed to be circumferentially uniform while the surface temperature is permitted to vary, the hot spot would occur at  $\theta = 0^\circ$ .

#### SIMPLIFIED ANALYSIS FOR LARGE SPACINGS

Both from physical reasoning and from the results of the foregoing analysis, it has been demonstrated that circumferential variations become smaller and smaller as the spacing ratio  $s/r_0$  increases. With this in mind, it seems worthwhile to reanalyze the problem using a model which neglects circumferential variations; and then, by comparing the results with those of the complete formulation already presented, to find for what conditions the simplified analysis is valid.

A flow model having the property of angular symmetry with respect to a cylinder is an annulus surrounding the cylinder. The inner radius of the annulus is  $r_0$ , while the outer radius  $r^*$  is chosen so that the flow area is identical to that in the actual configuration. From Fig. 2(a), it is seen that the actual flow area associated with a given cylinder is composed of 12 of the blackened typical elements. So, equating areas as follows

$$\pi(r^{*2} - r_0^2) = 12 \left[ \frac{s^2}{2} \tan \frac{\pi}{6} - \pi \frac{r_0^2}{12} \right] \quad (30a)$$

there is obtained

$$r^* = \left( \frac{2\sqrt{3}}{\pi} \right)^{1/2} s. \quad (30b)$$

The velocity problem for such an annulus is described by

$$\frac{\partial^2 u}{\partial r^2} + \frac{1}{r} \frac{\partial u}{\partial r} = \frac{1}{\mu} \frac{dp}{dz} \quad (31a)$$

$$u(r_0) = 0, \quad \frac{\partial u}{\partial r}(r^*) = 0 \quad (31b)$$

It is easily verified by direct substitution that the solution for the velocity distribution is given by

$$\frac{u}{s^2 \left( -\frac{1}{\mu} \frac{dp}{dz} \right)} = \frac{\sqrt{3}}{\pi} \ln \frac{r}{r_0} - \frac{1}{4} \left[ \left( \frac{r}{s} \right)^2 - \left( \frac{r_0}{s} \right)^2 \right] \quad (32)$$

which is identical to the nonseries part of the more complete velocity solution (3). From this, the flow parameter  $M$  which has been defined in Eq. (4) can be evaluated to be

$$M = \frac{1}{2\pi} \ln \frac{r^*}{r_0} - \frac{3}{8\pi} + \frac{\sqrt{3}}{12} \left( \frac{r_0}{s} \right)^2 - \frac{\pi}{96} \left( \frac{r_0}{s} \right)^4 \quad (33)$$

Next, by modifying the governing Eq. (5) to apply to the annulus, the temperature distribution problem may be formulated as

$$\frac{\partial^2 T}{\partial r^2} + \frac{1}{r} \frac{\partial T}{\partial r} = \frac{Q/12k}{Ms^2} \left\{ \frac{\sqrt{3}}{\pi} \ln \frac{r}{r_0} - \frac{1}{4} \left[ \left( \frac{r}{s} \right)^2 - \left( \frac{r_0}{s} \right)^2 \right] \right\} \quad (34a)$$

$$T(r_0) = T_w, \quad \frac{\partial T}{\partial r}(r^*) = 0 \quad (34b)$$

E-725



From this, the solution for the temperature is found to be

$$T - T_w = \frac{Q/12k}{Ms^2} \left\{ \left[ \frac{\sqrt{3}}{4\pi} (r^2 + r_0^2) - \frac{1}{16} \frac{r_0^4}{s^2} - \frac{6Ms^2}{\pi} \right] \ln \frac{r}{r_0} - \frac{1}{64} \frac{(r^4 - r_0^4)}{s^2} + \left[ -\frac{\sqrt{3}}{4\pi} + \frac{1}{16} \left( \frac{r_0}{s} \right)^2 \right] (r^2 - r_0^2) \right\} \quad (35)$$

It may be seen by inspection that this result is identical to the nonseries portion of the more complete temperature solution (15).

To compare the overall heat transfer characteristics with those previously obtained, we compute the wall-to-bulk temperature difference. Applying the definition of the bulk temperature from Eq. (21) to the annulus, there is obtained,

$$T_w - T_b = \frac{2\pi\rho \int_{r_0}^{r^*} (T_w - T)ur \, dr}{W} \quad (36)$$

By substituting from Eqs. (32) and (35), the integrand can be evaluated and then the integration carried out. The same type of functional relation which has been noted in Eq. (23) has also been found here. The end result of the calculation is reproduced in the Appendix to facilitate numerical calculations for  $s/r_0$  values which lie outside the range reported here.

With the wall-to-bulk temperature difference at our disposal, the Nusselt number  $Nu_d$  can be evaluated from Eq. (25). The results thus obtained have been plotted as a dotted line on Fig. 3 - left hand ordinate. By comparing with the solid curve from the more exact calculation, it is seen that the neglect of circumferential variations leads to a smaller wall-to-bulk temperature difference at a fixed heat transfer per unit length. So, for a given bulk temperature at a cross section, the wall temperature prediction from the simplified calculation is low. If errors up to 5 percent in the Nusselt number prediction can be tolerated, then from Fig. 3 it is found that the results based on the neglect of circumferential variations may be used for spacing

E-725

ratios as low as 1.5. As the spacing becomes progressively smaller, the deviations become increasingly larger. The same comments apply to the  $Nu_{de}$  curves associated with the right hand ordinate.

An analysis using the equivalent annulus approximation has been carried out in Ref. 3 for turbulent flow for spacings down to 1.375. If the flow is fully turbulent, then the effects of circumferential variations will likely be smaller than in a laminar flow. On this basis, we may conclude that the use of the equivalent annulus model appears justifiable in the turbulent case for the spacings considered in Ref. 3.

TABLE I. - LISTING OF  $\omega_j$  VALUES

$s/r_0$	$\omega_1 \times 10^2$	$\omega_2 \times 10^3$	$\omega_3 \times 10^5$	$\omega_4 \times 10^7$
4.0	2.9649	0.39239	0.579	~0.3
2.0	1.2712	.12031	.136	~.05
1.5	.71081	.014556	-.195	~-1.5
1.2	.37039	-.1323	-1.20	~-6.0
1.1	.25961	-.2065	-1.12	~7.0

REFERENCES

1. E. M. Sparrow and A. L. Loeffler, Jr., Longitudinal Laminar Flow Between Cylinders Arranged in Regular Array, A.I.Ch.E. Journal, vol. 5, pp. 325-329, 1959.
2. James P. Hartnett and Thomas F. Irvine, Jr., Nusselt Values for Estimating Turbulent Liquid Metal Heat Transfer in Noncircular Ducts, A.I.Ch.E. Journal, vol. 3, 1957, pp. 313-317.
3. O. E. Dwyer and P. S. Tu, Heat Transfer Rates for Parallel Flow of Liquid Metals Through Tube Bundles - I. A.I.Ch.E. Paper no. 119, 3rd National Heat Transfer Conference, 1959, Storrs, Connecticut.

CS/1-11

APPENDIX

(a) Integral table.

All integrals are over the range 0 to  $\pi/6$

$\int \theta \tan \theta \, d\theta = 0.05069781$	$\int (\ln \cos \theta) \cos 6\theta \, d\theta = 0.0150977$
$\int \frac{(\ln \cos \theta) \cos 6\theta \, d\theta}{(\cos \theta)^8} = 0.0370858$	$\int \frac{(\ln \cos \theta) \cos 12\theta \, d\theta}{(\cos \theta)^{14}} = -0.0434739$
$\int \frac{(\ln \cos \theta) \cos 6\theta \, d\theta}{(\cos \theta)^{10}} = 0.04655214$	$\int \frac{(\ln \cos \theta) \cos 12\theta \, d\theta}{(\cos \theta)^{16}} = -0.0577564$
$\int \frac{(\ln \cos \theta) \cos 6\theta \, d\theta}{(\cos \theta)^{-4}} = 0.00966175$	$\int \frac{(\ln \cos \theta) \cos 12\theta \, d\theta}{(\cos \theta)^{-10}} = 0.000874072$
$\int \frac{(\ln \cos \theta) \cos 6\theta \, d\theta}{(\cos \theta)^{-2}} = 0.01207813$	$\int \frac{(\ln \cos \theta) \cos 12\theta \, d\theta}{(\cos \theta)^{-8}} = 0.000413828$
$\int \frac{\cos 6\theta \, d\theta}{(\cos \theta)^8} = 0.195504853059$	$\int \frac{\cos 12\theta \, d\theta}{(\cos \theta)^{14}} = 0.24953325973$
$\int \frac{\cos 6\theta \, d\theta}{(\cos \theta)^{-4}} = 0.0487139289629$	$\int \frac{\cos 12\theta \, d\theta}{(\cos \theta)^{-10}} = 0.00934144946$
$\int \frac{\cos 6\theta \, d\theta}{(\cos \theta)^{10}} = -0.278775438621$	$\int \frac{\cos 12\theta \, d\theta}{(\cos \theta)^{16}} = 0.35013873273$
$\int \frac{\cos 6\theta \, d\theta}{(\cos \theta)^{-2}} = 0.0270632938683$	$\int \frac{\cos 12\theta \, d\theta}{(\cos \theta)^{-8}} = -0.01065617196$
$\int \frac{\cos 6\theta \, d\theta}{(\cos \theta)^{12}} = -0.3833738263351$	$\int \frac{\cos 12\theta \, d\theta}{(\cos \theta)^{18}} = 0.4834095306$
$\int \frac{\cos 12\theta \, d\theta}{(\cos \theta)^{-6}} = -0.01087364485$	$\int \frac{\cos 12\theta \, d\theta}{(\cos \theta)^2} = 0.00993262699$
$\int \frac{\cos 12\theta \, d\theta}{(\cos \theta)^4} = 0.02483882327$	$\int (\cos \theta)^8 \, d\theta = 0.37912963362$
$\int (\cos \theta)^{10} \, d\theta = 0.354917462776$	$\int (\cos \theta)^{-14} \, d\theta = 1.2290323215$
$\int (\cos \theta)^{-16} \, d\theta = 1.43544637803$	

(b) Wall-To-Bulk Temperature Difference For Equivalent Annulus

Let

$$\alpha = r_o/s, \quad \beta = \left[ \frac{2\sqrt{3}}{\pi} \right]^{1/2}$$

Then,

$$\begin{aligned} \frac{T_b - T_w}{(Q/12k)(\pi/6M^2)} &= \frac{3}{4\pi^2} \left[ \frac{\beta^4}{4} \left( \ln \frac{\beta}{\alpha} \right)^2 - \frac{1}{8} \beta^4 \left( \ln \frac{\beta}{\alpha} \right) + \frac{1}{32} \beta^4 - \frac{1}{32} \alpha^4 \right] \\ &+ \frac{\sqrt{3}}{\pi} \left[ -\frac{6M}{\pi} + \frac{\sqrt{3}}{4\pi} \alpha^2 - \frac{1}{16} \alpha^4 \right] \left[ \frac{\beta^2}{2} \left( \ln \frac{\beta}{\alpha} \right)^2 - \frac{\beta^2}{2} \left( \ln \frac{\beta}{\alpha} \right) + \frac{\beta^2}{4} - \frac{\alpha^2}{4} \right] \\ &\quad - \frac{5\sqrt{3}}{64\pi} \left[ \frac{\beta^6}{6} \left( \ln \frac{\beta}{\alpha} \right) - \frac{\beta^6}{36} + \frac{\alpha^6}{36} \right] + \frac{1}{2048} [\beta^8 - \alpha^8] \\ &\quad + \left[ -\frac{3}{4\pi^2} + \frac{\sqrt{3}}{16\pi} \alpha^2 + \frac{3M}{2\pi} + \frac{\alpha^4}{64} \right] \left[ \frac{\beta^4}{4} \left( \ln \frac{\beta}{\alpha} \right) - \frac{\beta^4}{16} + \frac{\alpha^4}{16} \right] \\ &\quad + \left[ \frac{3}{4\pi^2} \alpha^2 + \frac{\sqrt{3}}{64\pi} \alpha^4 - \frac{3M}{2\pi} \alpha^2 - \frac{1}{64} \alpha^6 \right] \left[ \frac{\beta^2}{2} \left( \ln \frac{\beta}{\alpha} \right) - \frac{\beta^2}{4} + \frac{\alpha^2}{4} \right] \\ &\quad + \left[ \frac{\sqrt{3}}{16\pi} - \frac{5}{256} \alpha^2 \right] \frac{(\beta^6 - \alpha^6)}{6} + \left( -\frac{\sqrt{3}}{8\pi} \alpha^2 + \frac{7}{256} \alpha^4 \right) \frac{(\beta^4 - \alpha^4)}{4} \\ &\quad + \left[ \frac{\sqrt{3}}{16\pi} \alpha^4 - \frac{3}{256} \alpha^6 \right] \frac{(\beta^2 - \alpha^2)}{2} \end{aligned}$$

E-725

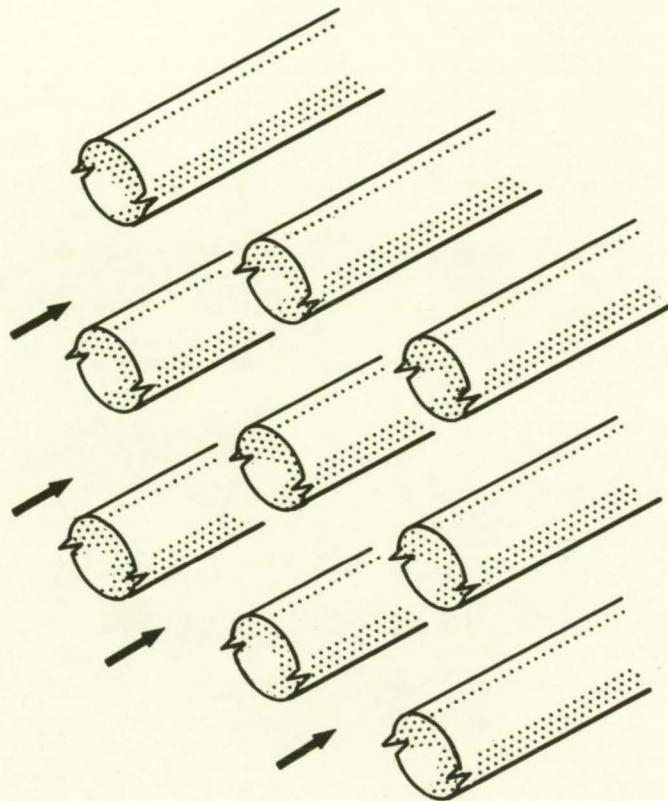


Figure 1. - Flow configuration.

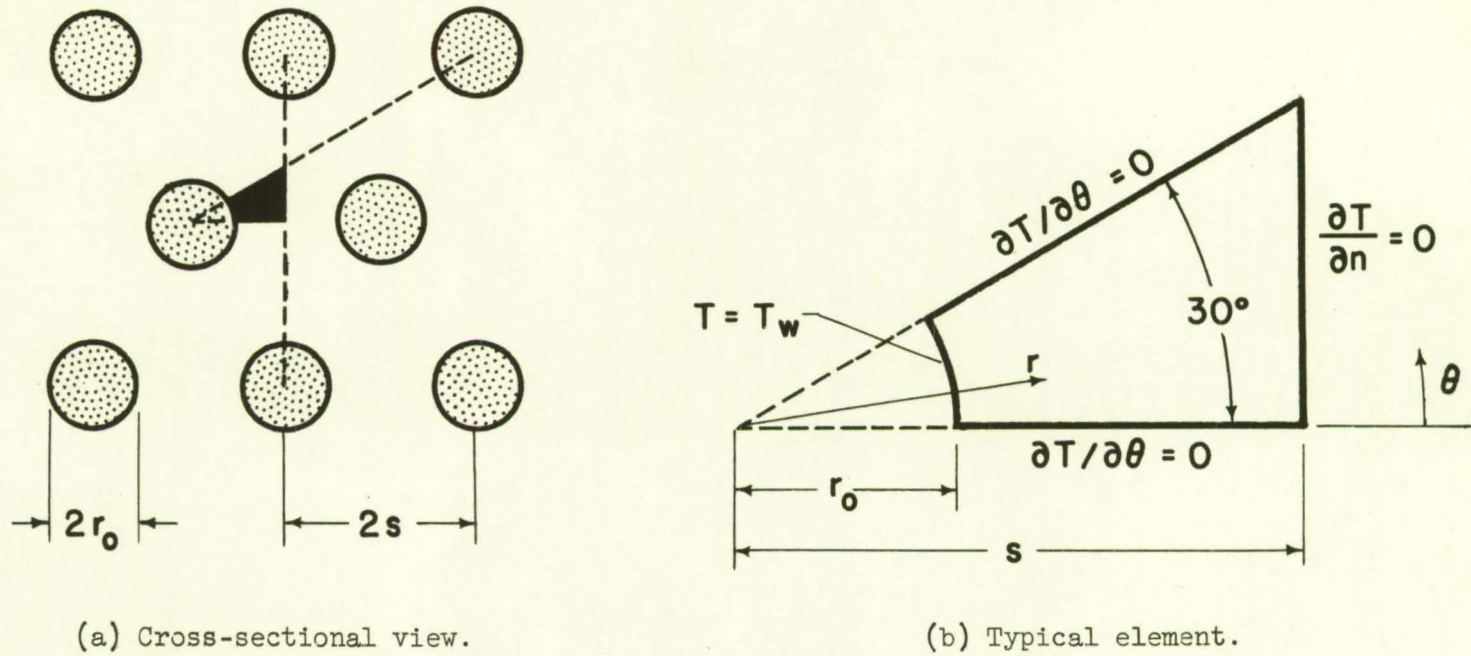


Figure 2. - Diagram used in mathematical formulation.

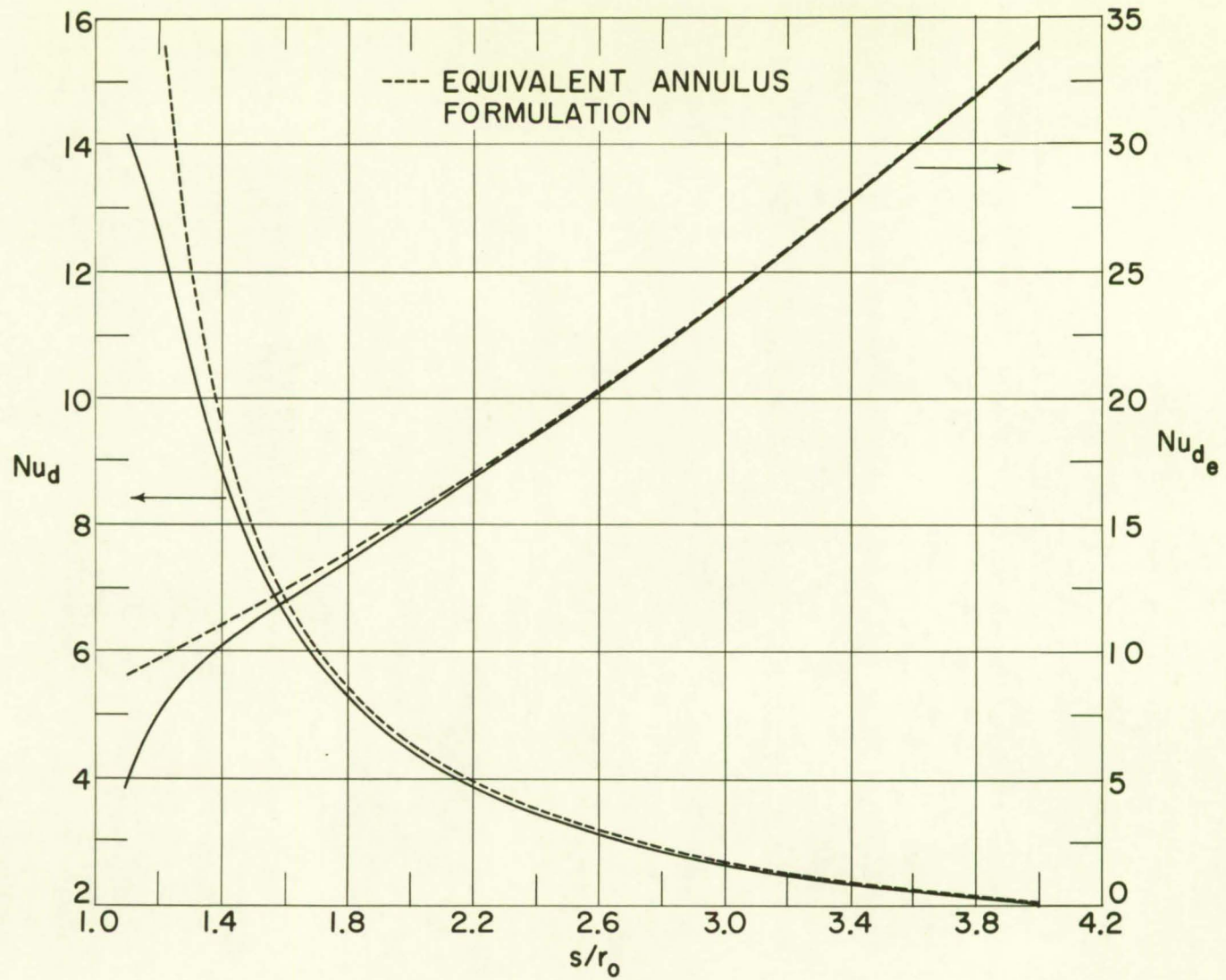


Figure 3. - Nusselt number results.

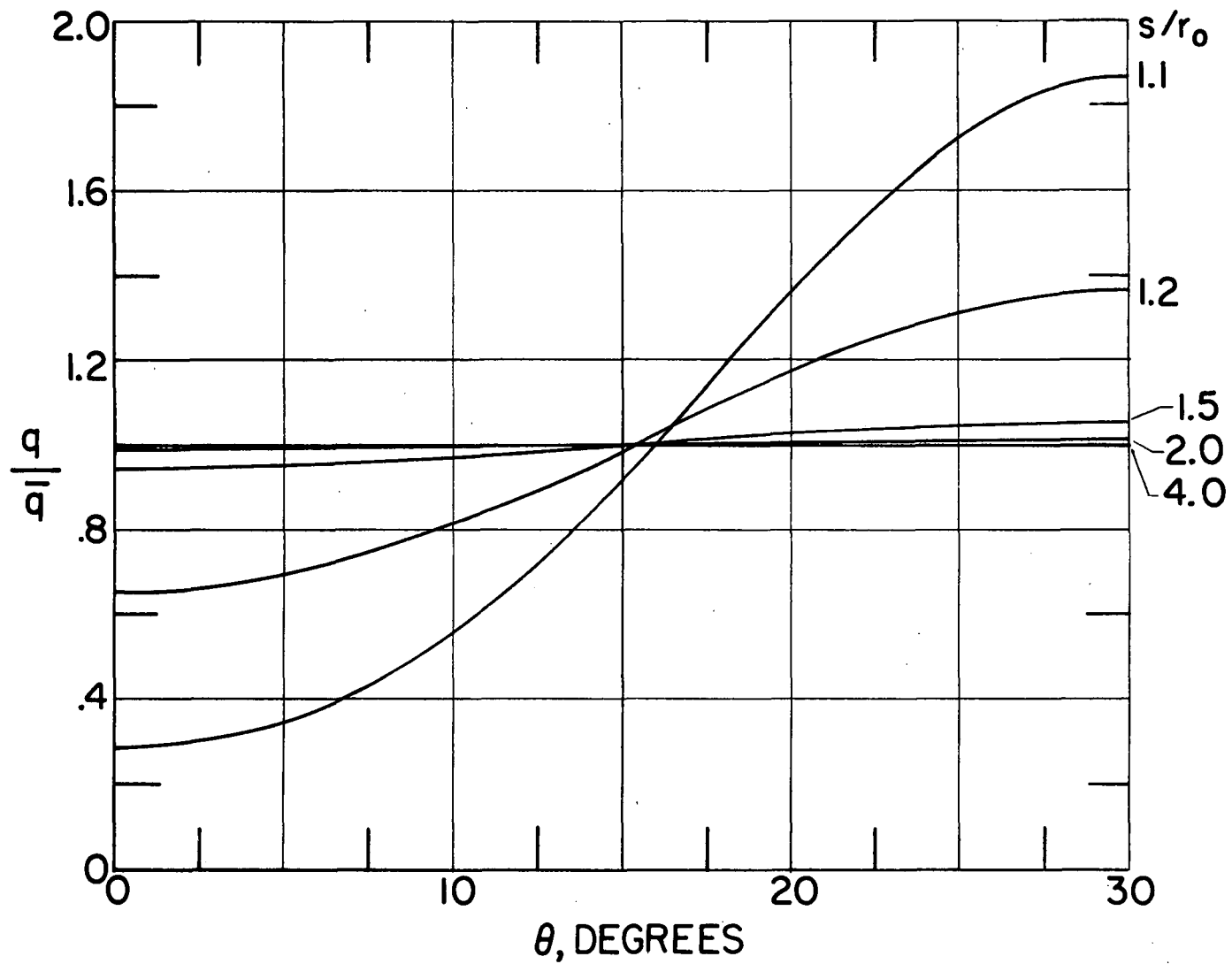


Figure 4. - Peripheral variation of wall heat transfer.



APR 4 1960

NASA FILE COPY  
loan expires on last  
date stamped on back cover.  
PLEASE RETURN TO  
DIVISION OF AERONAUTICS  
AND SPACE INFORMATION  
ADMINISTRATION  
Washington 25, D. C.